A theoretical study of X ligand effect on catalytic activity of complexes RuHX(diamine)(PPh_3)$_2$ (X = NCMe, CO, Cl, OMe, OPh, CCMe and H) in H_2-hydrogenation of ketones†

Zhuo Chen,[a] Yue Chen,[a] Yanhui Tang[b] and Ming Lei*[a]

Received 1st September 2009, Accepted 26th November 2009
First published as an Advance Article on the web 13th January 2010
DOI: 10.1039/b917934h

In this paper, the catalytic activities of RuHX(diamine)(PPh_3)$_2$ complexes with different X ligands (X = NCMe, CO, Cl, OMe, OPh, CCMe and H, corresponding catalytic processes are abbreviated in A, B, C, D, E, F and G systems, respectively) in the H_2-hydrogenation of ketones were investigated using density functional theory (DFT) method. Calculated results indicate that the rate-determining step in the whole catalytic cycle is hydrogen transfer (HT) for A–E but dihydrogen activation (DA) for F and G. The free energy barriers of the HT step for A–G are 36.1, 32.3, 21.2, 14.9, 21.9, 9.4 and 6.9 kcal mol^{-1}, respectively. The DA step consists of hydrogen coordination (HC) and hydrogen splitting (HS) steps if dihydrogen coordinates with the Ru center. The transition states (TSs) of H_2 coordinating with the Ru atom for A–G except B are located. The free energy barriers of DA for A–G are 17.8 (17.8, 2.6), 21.5, 12.8 (12.8, 3.8), 12.2 (11.2, 6.2), 13.6 (13.6, 4.1), 17.1 (9.7, 7.5) and 22.0 (10.4, 11.0) kcal mol^{-1}, respectively (the data in parentheses correspond to the barriers of HC and HS). HT barriers correlate well with the charges of hydride (H) in complex **1**. HC barriers are closely related to the Ru=N^1 double bond in **4**, and HS are in line with the proton-moved-distances (PMDs) from **5** to **TS5-1**. This study demonstrates that catalysts D, F and G show better catalytic activities than the others, which is in good agreement with experimental results.

Introduction

In the 1990s, Noyori and co-workers developed a novel, highly active and selective ruthenium catalyst with chiral phosphorous and diamine ligands for asymmetric hydrogenation of ketones.[1] Bearing electrophilic and nucleophilic sites, various late transition metal–ligand bifunctional catalysts were synthesized for enantioselective hydrogenation of polar bonds. The transition metals (TM), ligands and solvent used in catalysis could affect their catalytic activity and mechanism. Catalysts with different TM atoms like Os, Fe, Ir, Rh replacing Ru showed good activity in the hydrogenation of ketones.[2-7] Meanwhile, the ligand environment around the TM center involving X ligands *trans* to hydride, phosphorous and amine ligands were found to be strongly related to the catalysts' activity, enantiomeric excess (ee) of the chiral alcohol and yield.[8-16]

The hydrogenation of ketones could proceed *via* H_2-hydrogenation and transfer hydrogenation according to the usage of hydrogen resources. As shown in Scheme 1, the catalytic cycle of H_2-hydrogenation catalyzed by RuHX(diamine)(PPh_3)$_2$ could be divided into two parts: hydrogen transfer (HT) from **1** to the carbonyl group of ketones producing alcohols, and dihydrogen activation (DA) to reproduce active catalytic species from **4** to **1**. Acetone is used as the substrate in this study. In the first step, the carbon and oxygen atoms of the carbonyl group interact with H^1 (hydride) and H^2 (proton) of **1** respectively, forming **2** *via* a six-membered ring transition state (**TS2-3**). The DA process consists of two steps: hydrogen coordination (HC) and heterolytic hydrogen splitting (HS). In HC, dihydrogen coordinates with Ru in **4** *via* **TS4-5** forming a η^2-H_2 intermediate (**5**). Then, in HS, one hydrogen transfers to Ru as a hydride forming Ru–H^1 bond and the other to N^1 forming N^1–H^2 bond.

Dichloride precursors can be converted into the hydride species with HX (hydrogen gas, 2-propanol or strong base). Some monohydride complexes like RuHCl(diphosphine)(diamine) are inactive as ketone hydrogenation catalysts, but can be converted into active dihydride catalysts by reacting with a strong base and dihydrogen.[17] Meanwhile, some monohydride complexes like RuH(CCPh)(PPh_3)$_2$(diamine) are active catalysts in ketone hydrogenation without addition of base.[18] It is well known that the complex RuHX(diamine)(PPh_3)$_2$ using H and BH_4 as X ligands are intelligent catalysts for hydrogenation of ketones in the absence of base.[19,20] The RuHY(diamine)(PPh_3)$_2$ complexes with different Y ligands (Y = OPh, 4-$SC_6H_4OCH_3$, $OPPh_2$, $OP(OEt)_2$, CCPh, NCCHCN, $CH(COOMe)_2$) were studied experimentally and the one with CCPh ligand was found to be active for ketone hydrogenation reactions.[18] Although H_2-hydrogenation of ketones is not a common synthetic method to hydrogenate ketones compared to transfer hydrogenation, it is of importance to study

[a]*State Key Laboratory of Chemical Resource Engineering, Institute of Materia Medica, College of Science, Beijing University of Chemical Technology, Beijing, 100029, PR China. E-mail: leim@mail.buct.edu.cn; Fax: +86(10)64446598; Tel: +86(10)64446598*
[b]*School of Materials Science & Engineering, Beijing Institute of Fashion Technology, Beijing, 100029, PR China. E-mail: yanhui_tang@hotmail.com; Fax: +86(10)64284087; Tel: +86(10)64446598*

† Electronic supplementary information (ESI) available: Geometric structures of stationary points, structural changes along IRC paths of HT for seven systems, potential energy profiles, the relationship between NPA charge in complex **1** and HT barrier, calculated energies of all stationary points. See DOI: 10.1039/b917934h

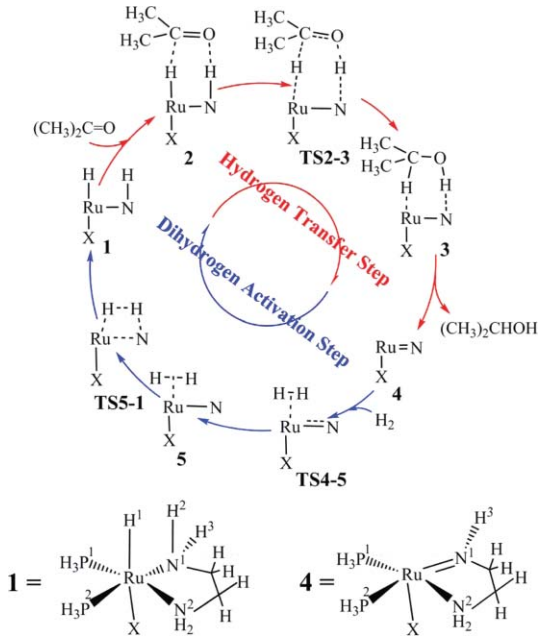

Scheme 1 Catalytic cycle of H_2-hydrogenation of ketones catalyzed by RuHX(diamine)$(PH_3)_2$. The red lines mean HT, and the blue ones are DA.

the modification effect of X-ligands *trans* to hydride of complex RuHX(diamine)$(PPh_3)_2$ in ketone hydrogenation. Here, the effect of X ligands (X = NCMe, CO, Cl, OMe, OPh, CCMe and H) on the catalytic activities of complex **1** in H_2-hydrogenation of ketones was investigated using DFT method. The calculated results indicate that complexes with a ligand which could weaken Ru–H^1 bond show good activity in both HT and HC, but they are relatively difficult to finish the HS step. The catalysts with OMe, CCMe and H ligand show better catalytic activities than the others.

Computational details

The effects of X ligands *trans* to the hydride of complexes RuHX(diamine)$(PPh_3)_2$ (X = NCMe, CO, Cl, OMe, OPh, CCMe and H, corresponding catalysts are abbreviated in A, B, C, D, E, F and G, respectively) in ketone hydrogenation were studied at B3LYP/BSI level. BSI denoted LANL2DZ basis set for Ru and 6-31+G** basis set for other atoms.[21-23] $\mathbf{1}_A$ represents catalytic species of RuHX(diamine)$(PPh_3)_2$ (**1**) with NCMe ligand. The hybrid density functional B3LYP method is reliable and was used in our previous papers.[24-26] The usage of BSI basis sets is useful to directly compare results with previous studies. The triphenylphosphine ligand (PPh_3) and diamine ligand were replaced by PH_3 and ethylenediamine for simplification, respectively. Active species **1** is an 18-electron complex, A and B (GI) have one unit of positive charge, C–G (GII) are electrically neutral. Because triplet states of **1** are 30–50 kcal mol^{-1} higher in energy than the singlet of **1**, all were calculated in singlet states. All calculations were carried out using Gaussian 03 program package.[27] Each transition state (**TS**) was confirmed by only one imaginary frequency. All energies reported in this paper are free energies if there are no other descriptions. Free energies were calculated at 298.15 K. The atomic polar tensor (APT) charge was calculated in this paper.[28] The solvent effect was also calculated using the polarizable continuum model (PCM) in the gas-phase optimized structures.[29] Methanol and benzene were used as solvents. The electronegativities of all atoms used Pauling scale.[30] Therefore, the electronegativities of ligand X_C and X_G are 3.16 and 2.20, respectively. The electronegativities of ligand X_A, X_D, X_E and X_F all come from the formula of the literature, and the electronegativity of ligand X_A is equal to 0.5 * {3.04 + 0.5 [2.55 + 0.25 (2.55 + 3 * 2.20)]}, namely 2.73.[31]

Results and discussion

The calculated structures of stationary points in the whole catalytic cycle for each system are shown in Fig. 1 and Table 1. In complex **1**, Ru–H^1 bonds are elongated to 1.607, 1.658, 1.616, 1.640, 1.622, 1.693 and 1.720 Å compared to normal Ru–H distances (1.60–1.65 Å) from A to G, respectively, but the N^1–H^2 and Ru–N^1 bond lengths had no obvious changes (around 1.017 and 2.216 Å, respectively). The charges of H^1 are –0.11, –0.087, –0.182, –0.204, –0.203, –0.238 and –0.268, respectively. The charges of Ru are –0.534, –0.737, –0.342, –0.326, –0.238, –0.623 and –0.671, respectively. When acetone approached complex **1** forming **2**, the bond lengths of Ru–H^1 and N^1–H^2 had little changes. (see Fig. 1). The charges on H^1 and Ru in $\mathbf{2}_{A-G}$ changed to –0.106, –0.085, –0.220, –0.243, –0.241, –0.277, –0.305, and –0.564, –0.765, –0.339, –0.323, –0.233, –0.619, –0.634, respectively. It is obvious that the X ligand affects bond lengths and charge population of Ru–H^1 bond in **1** and **2**. In amido intermediates $\mathbf{4}_{A-G}$, Ru=N^1 double bond lengths are 1.932, 1.942, 1.957, 1.982, 1.962 1.988 and 2.011 Å, respectively. While dihydrogen coordinated with Ru in **4** (except B) forming the η^2-H_2 intermediate **5**, the hybrid type of amido nitrogen changed from sp^2 to sp^3, because the sum of the three angles around the N^1 decreased from 356° to 327° and the Ru–N^1 distances increased to around 2.130 Å. The H^1–H^2 bond lengths are 0.818, 0.837, 0.828, 0.837, 0.794 and 0.778 Å (longer than normal H–H bond in H_2 molecule), for A and C–G, respectively. The charges on Ru changed from –0.318, –0.141, –0.114, –0.092, –0.415 and –0.430 to –0.518, –0.322, –0.306, –0.193, –0.630 and –0.587 for A and C–G respectively, while the charges on N^1 changed from –0.455, –0.519, –0.551, –0.516, –0.545 and –0.582 to –0.410, –0.455, –0.478, –0.462, –0.487 and –0.548 for A and C–G respectively. These results indicated that the double bond between the Ru atom and the amido nitrogen changed into a single bond after HC. In HS, the **TS5-1** had a four-membered ring structure Ru–H^1–H^2–N^1. The H^1–H^2 distances in $\mathbf{TS5\text{-}1}_{A-G}$ increased to 0.917, 0.898, 0.955, 0.974, 0.959, 0.977 and 1.000 Å, respectively, and the N^1–H^2 bond lengths decreased to 1.618, 1.572, 1.554, 1.489, 1.531, 1.440 and 1.389 Å, respectively (see Table 1).

The energy profiles along the catalytic reaction pathway for A–G are shown in Fig. 2 and Table 2. In HT, the barriers of F and G are 9.4 and 6.9 kcal mol^{-1}, respectively, but those for A–E are 36.1, 32.3, 21.2, 14.9 and 21.9 kcal mol^{-1}. DA consists of HC and HS steps if dihydrogen can coordinate with the Ru center. The free energy barriers of DA for A–G are 17.8, 21.5, 12.8, 12.2, 13.6, 17.1 and 22.0 kcal mol^{-1}, respectively. The barriers of HC for A and C–G are 17.8, 12.8, 11.2, 13.6, 9.7 and 10.4 kcal mol^{-1}, respectively. For B, the intermediate $\mathbf{5}_B$ could not be located. DA for B is predicted to be not involved with the HC step, the DA barrier of B is 21.5 kcal mol^{-1} from $\mathbf{4}_B$ to $\mathbf{TS5\text{-}1}_B$. The barriers of HS for A and C–G are 2.6, 3.8, 6.2, 4.1, 7.5 and 11.0 kcal mol^{-1},

Table 1 Selected bond lengths (Å) and charges (APT charge) of intermediates in the catalytic cycles

	Bond length/Å						Charge[b]							
	$Ru–H^1$ in **1**	$Ru=N^1$ in **4**	$H^1–H^2$ in **5**	$H^1–H^2$ in **TS5-1**	$N^1–H^2$ in **TS5-1**	PMDs[a]	Ru in **1**	H^1 in **1**	Ru in **2**	H^1 in **2**	Ru in **4**	Ru in **5**	N^1 in **5**	CD[b] in **5**
A	1.607	1.932	0.818	0.917	1.618	0.623	–0.534	–0.110	–0.564	–0.106	–0.318	–0.518	–0.410	0.064
B	1.658	1.942	—	0.898	1.572	—	–0.737	–0.087	–0.765	–0.085	—	—	—	—
C	1.616	1.957	0.837	0.955	1.554	0.734	–0.342	–0.182	–0.339	–0.220	–0.141	–0.322	–0.455	0.060
D	1.640	1.982	0.828	0.974	1.489	0.833	–0.326	–0.204	–0.323	–0.243	–0.114	–0.306	–0.478	0.052
E	1.622	1.962	0.837	0.959	1.531	0.737	–0.238	–0.203	–0.233	–0.241	–0.092	–0.193	–0.462	0.063
F	1.693	1.988	0.794	0.977	1.440	0.940	–0.623	–0.238	–0.619	–0.277	–0.415	–0.630	–0.487	0.045
G	1.720	2.011	0.778	1.000	1.389	1.072	–0.671	–0.268	–0.634	–0.305	–0.430	–0.587	–0.548	0.030

[a] Proton-moved-distances from **5** to **TS5-1**. [b] Charge difference between H^2 and H^1.

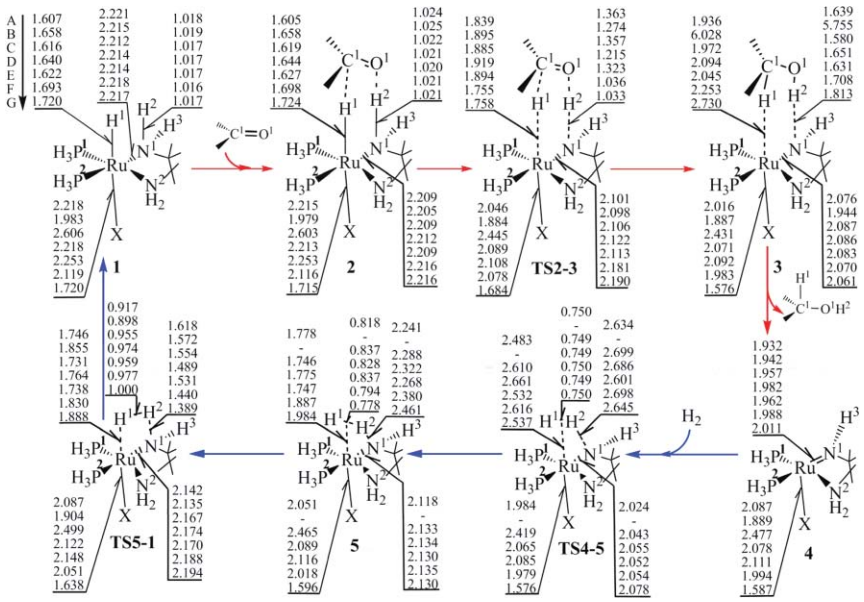

Fig. 1 Geometrical structures of Ru catalysts with different X ligands along reaction pathway. (Bond lengths are in Å, data from top to bottom correspond to those from A–G, respectively.)

respectively. Results imply that the barriers of DA for F and G are high enough to be the rate-determining step, but the HT step is the rate-determining step for the other systems.

In our previous study on the effect of the TM centre on the catalytic activity, we found three hydrogen transfer modes: (1) hydride transfer precedes proton transfer; (2) hydride and proton transfer synchronously; (3) proton transfer precedes hydride transfer. Different hydrogen transfer modes illustrate different barriers – the barrier of mode 1 is much lower than that of mode 2.[25] According to frontier orbital theory, GI and GII belong to mode 2 and mode 1, respectively (see Fig. S1, ESI†). Consequently, the barriers of HT in GI are much higher than those in GII. The HT barriers are closely related to the strength of $Ru–H^1$ in **1** or **2**. While the $Ru–H^1$ bond lengths in complex **1** became longer, the HT barriers would decrease gradually (see Fig. 3a). For A, $Ru–H^1$ bond length is the shortest, so its HT barrier is the highest. Interestingly, the reverse is true of G. In general, the stronger bond strength of $Ru–H^1$ leads to the higher barrier of HT. This is consistent with previous experimental and theoretical studies.[18,25] Fig. 3b showed the correlation between the APT charges of H^1 in complex **1** and HT barriers. This correlation has similar tendency using NPA charge compared with that using APT charge as shown in Fig. S3, ESI.† It implies that, the more negative charge H^1 has, the lower the barrier is. In other words, an increase on the basicity of H^1 in complex **1** will make the HT easier.

The X ligand plays an important role in HT among all systems, which affects the $Ru–H^1$ bond lengths and the charges of H^1 in **1**. Coe and Glenwright had pointed out that the kinetic *trans*-effect (TE) of X ligand was determined primarily by the electronic effects and decreased with the metal centre becoming less electron-rich.[32] The charges of Ru in $\mathbf{1}_{A–G}$ are –0.534, –0.737, –0.342, –0.326, –0.238, –0.623 and –0.671, respectively (see Table 1). Therefore, there are high TE of X ligands *trans* to the $Ru–H^1$ bonds in $\mathbf{1}_B$, $\mathbf{1}_F$ and $\mathbf{1}_G$. On the other hand, the electronegative coordinating ions like $X_{C–G}$ ligands have a greater labilizing effect on the group in the *trans* position than neutral ligands like X_A and X_B ligands.[33] As shown in Table 1, the bond lengths of $Ru–H^1$ in $\mathbf{1}_{A–G}$ can be attributed to the TE of X ligand (1.607, 1.658, 1.616, 1.640, 1.622, 1.693 and 1.720 Å, respectively). The $Ru–H^1$ bond length in **1** could be used as a measure of the TE of X ligand in the HC and HS steps. The bond lengths of $Ru–H^1$ in $\mathbf{1}_F$ and $\mathbf{1}_G$ are much longer than those in $\mathbf{1}_{A–E}$, where the $Ru–H^1$ bond length in $\mathbf{1}_B$ is

Table 2 The relative energies of intermediates in the catalytic cycles

	A	B	C	D	E	F	G
1[a]	0.0	0.0	0.0	0.0	0.0	0.0	0.0
	0.0	0.0	0.0	0.0	0.0	0.0	0.0
	0.0	0.0	0.0	0.0	0.0	0.0	0.0
2[b]	0.5	–0.5	7.0	7.7	5.5	7.2	6.1
	1.9	1.3	2.2	2.8	2.6	3.2	3.4
	–3.6	–4.8	–1.1	–0.8	–0.8	–1.1	–1.6
TS2-3[b]	36.6	31.7	28.2	22.7	27.5	16.6	13.0
	27.1	23.8	23.4	13.8	19.6	8.8	6.6
	25.6	22.0	18.2	11.6	16.6	4.7	1.2
3[b]	37.9	15.4	29.3	22.9	27.9	11.8	–0.4
	26.8	13.6	23.4	13.8	19.5	4.8	–5.1
	25.1	8.4	18.0	10.4	16.0	–0.1	–11.2
4[c]	21.5	15.2	21.3	16.3	18.8	5.7	–4.3
	19.6	13.7	20.6	14.0	17.0	4.8	–3.6
	19.3	13.5	19.9	14.1	17.0	3.5	–6.6
TS4-5[d]	39.2	—	34.1	27.5	32.4	15.4	6.1
	29.5	—	28.9	19.0	24.5	9.3	0.3
	29.2	—	25.5	17.4	22.6	6.3	–3.8
5[d]	35.6	—	28.4	22.3	26.9	15.3	6.8
	20.8	—	17.7	9.6	14.2	4.3	–2.3
	22.0	—	16.0	9.0	13.6	2.4	–5.6
TS5-1[d]	38.2	36.7	32.2	28.5	31.0	22.9	17.8
	25.8	26.5	23.6	18.1	21.0	14.9	9.9
	25.5	25.7	21.1	16.4	19.0	11.5	5.9
1[d]	–0.6	–0.6	–0.6	–0.6	–0.6	–0.6	–0.6
	–18.4	–18.4	–18.4	–18.4	–18.4	–18.4	–18.4
	–17.5	–17.5	–17.5	–17.5	–17.5	–17.5	–17.5
ΔX_{HT}[e]	36.1	32.3	21.2	14.9	21.9	9.4	6.9
	25.2	22.5	21.2	11.0	17.1	5.6	3.2
	29.2	26.8	19.3	12.4	17.3	5.8	2.8
ΔX_{HC}[e]	17.8	—	12.8	11.2	13.6	9.7	10.4
	9.9	—	8.3	4.9	7.5	4.5	3.9
	9.9	—	5.6	3.3	5.7	2.9	2.8
ΔX_{HS}[e]	2.6	—	3.8	6.2	4.1	7.5	11.0
	4.9	—	5.9	8.5	6.9	10.7	12.2
	3.6	—	5.1	7.4	5.4	9.1	11.5

All of the systems (A–G) have three rows of data. The first row gives the relative free energies in the gas phase, the second row gives potential energies in methanol, and the third row gives relative potential energies in benzene.[a] **1** + actone + H_2. [b] **2** + H_2, **TS2-3** + H_2, **3** + H_2. [c] **4** + 2-propanol + H_2. [d] **TS4-5** + 2-propanol, **5** + 2-propanol, **TS5-1** + 2-propanol, **1** + 2-propanol. [e] ΔX_{HT}, ΔX_{HC} and ΔX_{HS} are the free energy barriers ΔG (first row) and potential energy barriers ΔE^{sol} in solvents (the second and third row) of HT, HC and HS, respectively, unit: kcal mol^{-1}.

longer than that in $\mathbf{1}_A$, $\mathbf{1}_{C-E}$. However, H^1 in $\mathbf{1}_B$ owns the minimal negative charge (see Fig. 3b and Table 1). This may explain that $\mathbf{1}_B$ has a high barrier of HT with a long Ru–H^1 bond length in Fig. 3a. Complexes $\mathbf{1}_F$ and $\mathbf{1}_G$ showed the best catalytic activity in HT according to the two factors above because they contain the longest Ru–H^1 bond lengths and the most negative charges of H^1 in complex **1**. $\mathbf{1}_D$ is predicted to be active in hydrogenation of ketones based on its relatively low HT barrier. On the contrary, the hydrogenation of ketones for A, B, C and E would become difficult with high HT barriers.

In HC, the Ru=N^1 π-bond was broken with the coordination of dihydrogen, which could provide a vacant d-orbital to accommodate the dihydrogen coordinating with Ru.[34] The three-dimension (3D) Fig. 4a shows the correlation among the electronegativities of X ligands (for A, C–G are 2.73, 3.16, 2.86, 2.94, 2.48 and 2.20, respectively),[31] Ru=N^1 double bond lengths in **4**, and the HC barriers. It is obvious that the longer the Ru=N^1 double bond length is, the lower the barrier is. It is to say that the strength of Ru=N^1 is one of the key factors which affects the HC barrier. There is a relationship between the Ru=N^1 double bond length and the electronegativity of X ligand. The less electronegative they are, the longer the Ru=N^1 bond length. The HC barriers increase with the electronegativities of X ligand. (A is not included and will be discussed later.) As mentioned in HT, the stronger TE of X ligands will lead to longer Ru–H^1 bond lengths in **1** or **2** (see Fig. 3a). Therefore, it is easier for C–G systems to finish HC than that in A (see Fig. 4b). The HC barrier is related with a joint effect of the electronegativities and TE of X ligands. For A system, the electronegativity of X ligand in **4** is not the maximal, it could be understandable that the HC barrier of A is the highest due to its low TE of X ligand. And the HC barriers for F and G are low because X_F and X_G own a weak electronegativity and a strong TE.

Following HC, HS is a heterolytic H–H cleavage process in which one hydrogen atom H^1 transfers to Ru as a hydride and the other hydrogen atom H^2 transfers to N^1 as a proton. The amplitudes of imaginary frequencies of **TS5-1** come mainly from the vibration of proton (H^2) between the N^1 and H^2, while the vibration of H^1 has little contribution. From **5** to **TS5-1**, the main changes of structures are the distance between H^2 and N^1 (see Fig. 1). As shown in Table 1, the N^1–H^2 bond lengths decreasing for D, F and G are much longer than those for A, C and E (N^1–H^2 distances in D, F and G decreased by 0.833, 0.940 and 1.072 Å, respectively, and those in A, C and E decreased by 0.623, 0.734, and 0.737 Å, respectively). These indicate that the proton in D, F and G must move longer distances to finish HS than those in the others, and more energies are required. Fig. 5a shows that the barriers will grow with the proton-moved-distances (PMDs) from **5** to **TS5-1**. Similarly, it is found that the HS barrier is affected by the TE of X ligand (the stronger the TE is, the higher the HS barrier is). Meanwhile, the TE affects the distance between Ru and dihydrogen in **5**. The distances between Ru and dihydrogen for A, C–G are 1.778, 1.746, 1.775, 1.747, 1.887 and 1.984 Å, respectively. The distances in C–E are shorter than those in A, F and G due to the electronic effect of the atom of X ligands *trans* to dihydrogen. The charges of the atoms *trans* to dihydrogen bonding with Ru are 0.121, –0.520, –0.710, –1.001, 0.046 and –0.086 for A and C–G respectively. Apparently, the atom *trans* to dihydrogen in $\mathbf{5}_{C-E}$ own much more negative charges than that in the others. As a result, Ru centers for C–E have less negative charges (–0.322, –0.306 and –0.193 respectively) than those in A, F and G (–0.518, –0630 and –0.587, respectively). As mentioned above that the kinetic TE of X ligand was determined primarily by the electronic effects and decreased with the metal centre becoming less electron-rich, the negative ligands have a more labilizing effect on the group in the *trans* position than neutral ligands. Therefore, the distances between Ru and dihydrogen can be attributed to the TE of X ligands. As the distances decrease, the H^1–H^2 bond length in **5** will increase, and the polarity (charge difference) between them will increase gradually (see Table 1), the interaction between hydride and proton becomes weaker. Thus, the less energy is required to split the H^1–H^2 bond. As shown in Fig. 5b, the charge difference between H^2 and H^1 (CD) in **5** is influenced by the TE of X ligand, which are both related to the HS barriers. As the TE of X ligand decreases, the H^2–H^1 bond is gradually becoming an "electrovalent" bond. Thus a weaken polarity of H^1–H^2 bond will lead to a higher HS barrier. The discussion above showed that

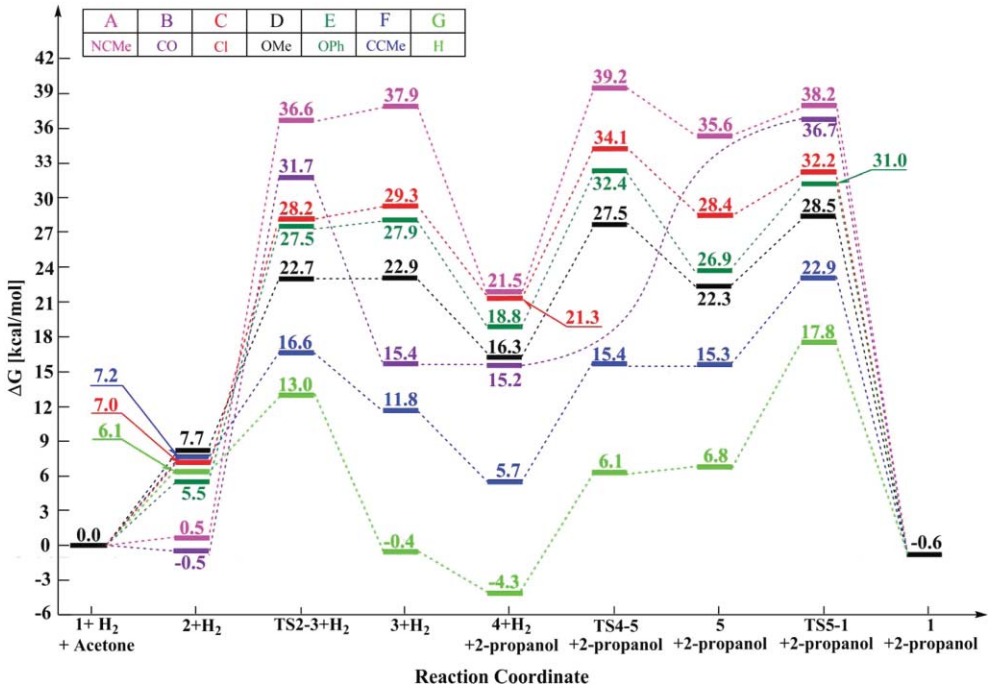

Fig. 2 Free energy profiles of H_2-hydrogenation of ketones for A–G (in kcal mol^{-1}).

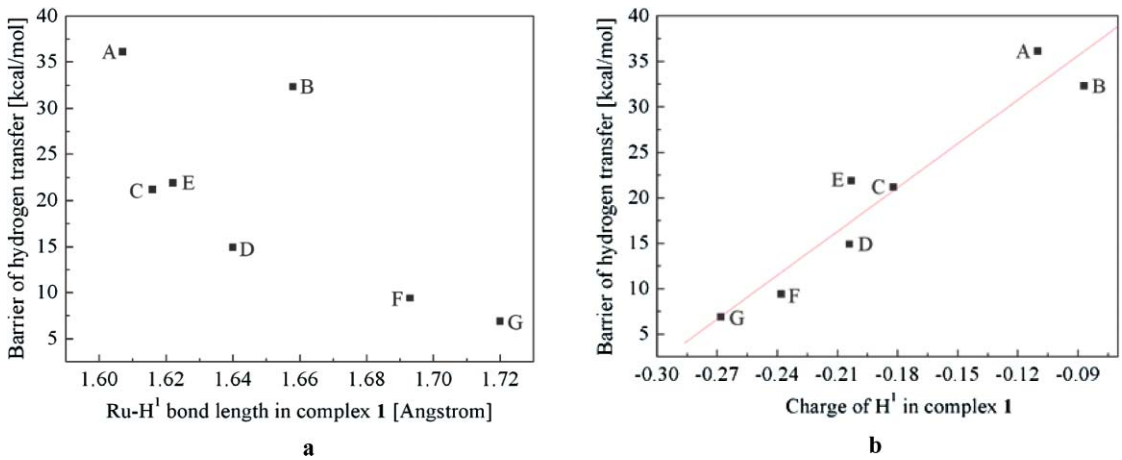

Fig. 3 (a) Correlation between the Ru–H^1 bond length in complex **1** and barrier of hydrogen transfer; (b) correlation between the H^1 charge in complex **1** and barrier of hydrogen transfer (coefficient of linear fit regression is 0.958).

the barrier of HS depended on the balance between two factors, PMDs from **5** to **TS5-1** and CD in **5**. They are both influenced by the TE of X ligand. In F and G, the PMDs are the longest (0.940 and 1.072 Å, respectively), and they own the weakest polarities in H^1–H^2 bond (0.045 and 0.030, respectively). Consequently, it could be predicted that the HS barriers for F and G are much higher than the others.

As discussed above, the barriers of HT, HC and HS are all affected by the TE of X ligand. In HT, the complex with a high TE of X ligand has a longer Ru–H^1 bond length and more negative charge of H^1 in complex **1**, which makes hydrogen transfer easier. In HC, the systems with low *trans* influence ligand in **4** will need more energy to finish dihydrogen coordination with the Ru centre. In HS, high TE ligand tends to increase PMDs and decrease the H^1–H^2 bond polarities, which make H^1–H^2 cleavage more difficult. On the other hand, HS could be regarded as the reverse process of HT. In HT, H^1 and H^2 transfer to the ketones from Ru and N^1, respectively. However, in HS, they come back again to the Ru and N^1, respectively. Therefore, high TE ligand will be helpful for HT and HC steps but not for HS step as shown in Fig. 6.

We also noticed that RuH(CCPh)(diamine)$(PPh_3)_2$ similar to $\mathbf{1}_F$ was not observed in experimental studies, it was proposed that it could convert into complex $\mathbf{1}_G$ under 1 atm H_2 (eqn (1)) during the catalytic reaction.[18] As shown in Fig. 7, we assumed that complex $\mathbf{1}_F$ firstly eliminated one molecule HCCMe forming intermediate $\mathbf{4}_G$ *via* $\mathbf{TS1}_F$-$\mathbf{4}_G$ (barrier is 22.8 kcal mol^{-1}, imaginary

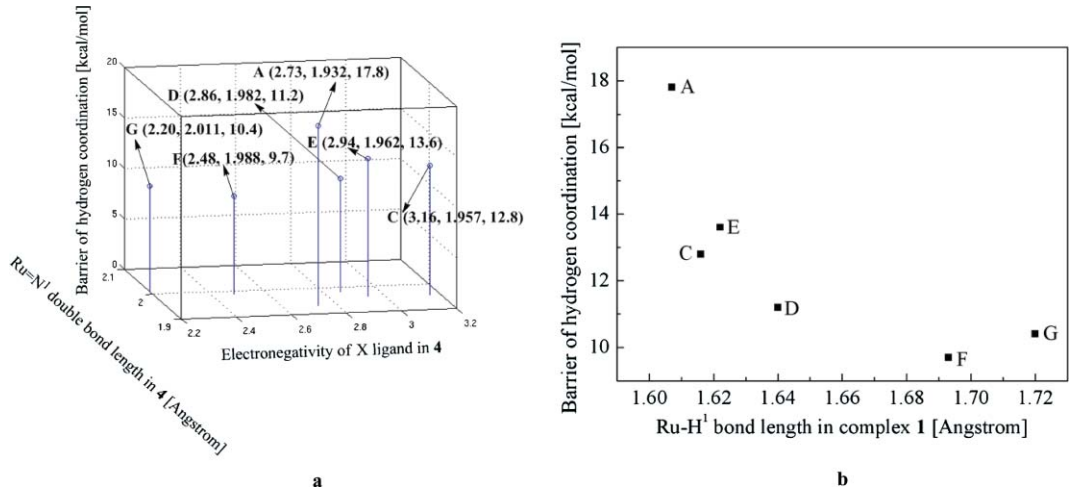

Fig. 4 (a) Three-dimension graph of electronegativity of X ligand, Ru=N^1 double bond length in **4**, and barrier of HC; (b) correlation between the Ru–H^1 bond length in complex **1** and barrier of HC.

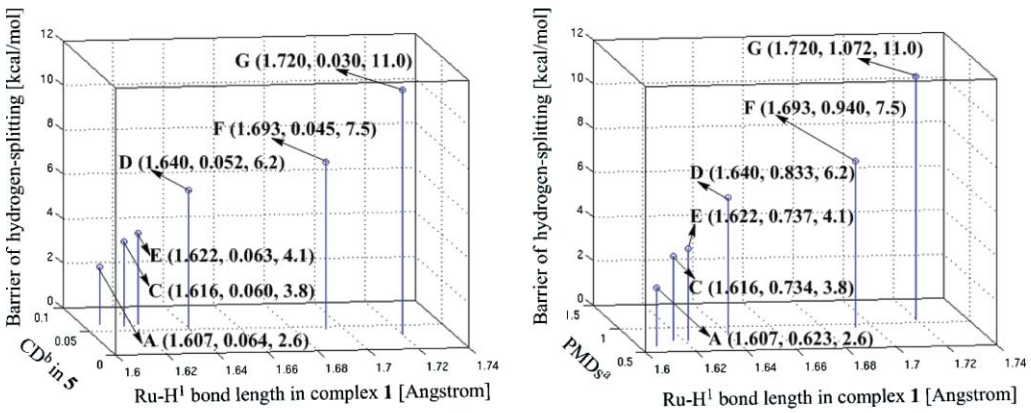

Fig. 5 (a) Three-dimension graph of Ru–H^1 bond length in **1**, PMDs and barrier of HS; (b) three-dimension graph of Ru–H^1 bond length in **1**, CD in **5** and barrier of HS. [a]Proton-moved-distances (PMDs) from **5** to **TS5-1** (Angstrom). [b]Charge difference between H^2 and H^1.

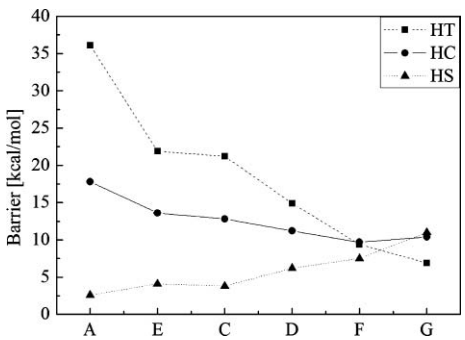

Fig. 6 The calculated barriers of HT, HC and HS steps in the catalytic cycle.

frequency is 1258.8 *i*), then $\mathbf{4}_G$ finished DA to produce complex $\mathbf{1}_G$. The results demonstrate that this transformation from $\mathbf{1}_F$ to $\mathbf{1}_G$ is not a favorable path compared with the hydrogen transfer reaction (HT barrier for F is only 9.4 kcal mol^{-1}) under room temperature. But $\mathbf{1}_F$ could be likely to convert into $\mathbf{1}_G$ under a high temperature.

$$\mathbf{1}_F + H_2 \rightarrow \mathbf{1}_G + HCCMe + \text{unidentified products} \quad (1)$$

The catalytic reactions were carried out in solvent (alcohols usually), and the solvent effects in two solvents (methanol and benzene) were calculated single point potential energies using PCM based on the optimized structures in vacuum (see Table 2). For GI, the barriers of HT decrease about 6 and 2 kcal mol^{-1} in benzene and methanol, respectively, and those for C and E increase less than 3 kcal mol^{-1}, and those for D, F and G decrease less than 2 kcal mol^{-1}. The barriers of HC for A increase by 0.1 kcal mol^{-1} in two solvents, and those for GII increase by within 4 kcal mol^{-1}. The barrier of HS, for all the systems, increase by less than 2 kcal mol^{-1} in two solvents. It is clear that no matter in vacuum or solvents to finish the catalytic cycles of ketone hydrogenation are very difficult for A and B because of their high HT barriers. In general, the results in the gas-phase above are reliable even considering the solvent effect.

Conclusion

In summary, seven systems with different X ligands for H_2-hydrogenation of ketones were compared using DFT method.

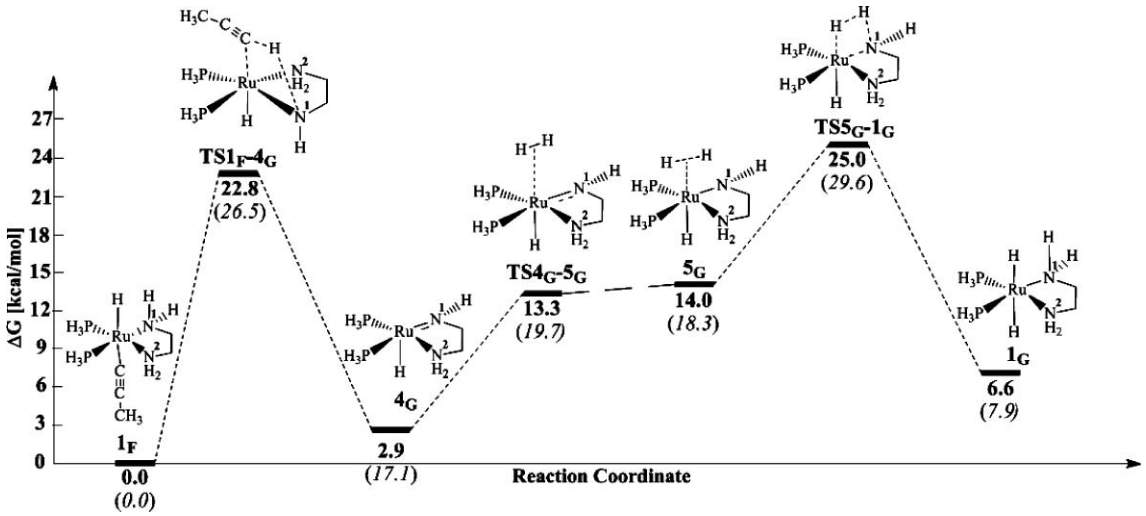

Fig. 7 Energy profiles of eqn (1). **Bold text**: the free energy, In *italics*: the potential energy (without zero-point energy correction).

Calculated results indicate that the rate-determining step in the whole catalytic cycle vary for A–G; hydrogen transfer (HT) for A–E, but dihydrogen activation (DA) for F and G. The energy barriers of HT for A–G are 36.1, 32.3, 21.2, 14.9, 21.9, 9.4 and 6.9 kcal mol^{-1}, respectively. DA consists of hydrogen coordination (HC) and hydrogen splitting (HS). The DA barriers for A–G are 17.8 (17.8, 2.6), 21.5 (NA, NA), 12.8 (12.8, 3.8), 12.2 (11.2, 6.2), 13.6 (13.6, 4.1), 17.1 (9.7, 7.5) and 22.0 (10.4, 11.0) kcal mol^{-1}, respectively (the data in parentheses correspond to HC and HS barriers). The barriers of HT and DA are closely related to the *trans*-effect (TE) of X ligand. In HC, the barrier was also influenced by the electronegativity of X ligand. In HS, bond polarity (charge difference) of H^1–H^2 in **5** and the PMDs from **5** to **TS5-1** both affect the barriers of HS. These also can be due to the TE of X ligands. A strong *trans* influence ligand X in catalysts show better catalytic activities than the low ones like A and B. Complexes with the ligand which could weaken Ru–H^1 bond will show good activity in both HT and HC processes, but it is relatively difficult to finish HS for them. The calculated results indicate that the catalysts with OMe, CCMe and H ligand show better catalytic activities in H_2 hydrogenation of ketones to alcohols.

Acknowledgements

This work was supported by Beijing Nova Fund (2005B17), the National Natural Science Foundation of China (Grant 20703003). We also thank Chemical Grid Project at Beijing University of Chemical Technology (BUCT) for providing part of the computational resources.

Notes and references

1 T. Ohkuma, H. Ooka, T. Ikariya and R. Noyori, *J. Am. Chem. Soc.*, 1995, **117**, 10417.
2 S. E. Clapham and R. H. Morris, *Organometallics*, 2005, **24**, 479.
3 C. Sui-Seng, F. Freutel, A. J. Lough and R. H. Morris, *Angew. Chem., Int. Ed.*, 2008, **47**, 940.
4 A. A. Mikhailine, E. Kim, C. Dingels, A. J. Lough and R. H. Morris, *Inorg. Chem.*, 2008, **47**, 6587.
5 A. A. Mikhailine, A. J. Lough and R. H. Morris, *J. Am. Chem. Soc.*, 2009, **131**, 1394.
6 M. J. Palmer and M. Wills, *Tetrahedron: Asymmetry*, 1999, **10**, 2045.
7 M. Torrent, M. Sola and G. Frenking, *Chem. Rev.*, 2000, **100**, 439.
8 S. Hashiguchi, A. Fujii, J. Takehara, T. Ikariya and R. Noyori, *J. Am. Chem. Soc.*, 1995, **117**, 7562.
9 R. Noyori and S. Hashiguchi, *Acc. Chem. Res.*, 1997, **30**, 97–102.
10 K. Abdur-Rashid, M. Faatz, A. J. Lough and R. H. Morris, *J. Am. Chem. Soc.*, 2001, **123**, 7473.
11 R. Noyori and T. Ohkuma, *Angew. Chem., Int. Ed.*, 2001, **40**, 40.
12 T. Ohkuma, M. Koizumi, K. Muniz, G. Hilt, C. Kabuto and R. Noyori, *J. Am. Chem. Soc.*, 2002, **124**, 6508.
13 T. Ohkuma, C. A. Sandoval, R. Srinivasan, Q. Lin, Y. Wei, K. Muniz and R. Noyori, *J. Am. Chem. Soc.*, 2005, **127**, 8288.
14 S. Gladiali and E. Alberico, *Chem. Soc. Rev.*, 2006, **35**, 226.
15 T. Ikariya and A. J. Blacker, *Acc. Chem. Res.*, 2007, **40**, 1300.
16 D. S. Matharu, J. E. D. Martins and M. Wills, *Chem.–Asian J.*, 2008, **3**, 1374.
17 R. Abbel, K. Abdur-Rashid, M. Faatz, A. Hadzovic, A. J. Lough and R. H. Morris, *J. Am. Chem. Soc.*, 2005, **127**, 1870.
18 S. E. Clapham, R. Guo, M. Z.-D. Iuliis, N. Rasool, A. J. Lough and R. H. Morris, *Organometallics*, 2006, **25**, 5477.
19 K. Abdur-Rashid, S. E. Clapham, A. Hadzovic, J. N. Harvey, A. J. Lough and R. H. Morris, *J. Am. Chem. Soc.*, 2002, **124**, 15104.
20 C. A. Sandoval, T. Ohkuma, K. Muniz and R. Noyori, *J. Am. Chem. Soc.*, 2003, **125**, 13490.
21 D. B. Axel, *J. Chem. Phys.*, 1993, **98**, 5648.
22 C. Lee, W. Yang and R. G. Parr, *Phys. Rev. B*, 1988, **37**, 785.
23 P. J. Hay and R. W. Willard, *J. Chem. Phys.*, 1985, **82**, 299.
24 Y. Chen, Y. Tang, S. Liu, M. Lei and W. Fang, *Organometallics*, 2009, **28**, 2078.
25 Y. Chen, Y. Tang and M. Lei, *Dalton Trans.*, 2009, 2359.
26 Y. Chen, S. Liu and M. Lei, *J. Phys. Chem. C*, 2008, **112**, 13524.
27 M. J. Frisch, G. W. Trucks, H. B. Schlegel, G. E. Scuseria, M. A. Robb, J. R. Cheeseman, J. A. Montgomery, Jr., T. Vreven, K. N. Kudin, J. C. Burant, J. M. Millam, S. S. Iyengar, J. Tomasi, V. Barone, B. Mennucci, M. Cossi, G. Scalmani, N. Rega, G. A. Petersson, H. Nakatsuji, M. Hada, M. Ehara, K. Toyota, R. Fukuda, J. Hasegawa, M. Ishida, T. Nakajima, Y. Honda, O. Kitao, H. Nakai, M. Klene, X. Li, J. E. Knox, H. P. Hratchian, J. B. Cross, V. Bakken, C. Adamo, J. Jaramillo, R. Gomperts, R. E. Stratmann, O. Yazyev, A. J. Austin, R. Cammi, C. Pomelli, J. Ochterski, P. Y. Ayala, K. Morokuma, G. A. Voth, P. Salvador, J. J. Dannenberg, V. G. Zakrzewski, S. Dapprich, A. D. Daniels, M. C. Strain, O. Farkas, D. K. Malick, A. D. Rabuck, K. Raghavachari, J. B. Foresman, J. V. Ortiz, Q. Cui, A. G. Baboul, S. Clifford, J. Cioslowski, B. B. Stefanov, G. Liu, A. Liashenko, P.

Piskorz, I. Komaromi, R. L. Martin, D. J. Fox, T. Keith, M. A. Al-Laham, C. Y. Peng, A. Nanayakkara, M. Challacombe, P. M. W. Gill, B. G. Johnson, W. Chen, M. W. Wong, C. Gonzalez and J. A. Pople, *GAUSSIAN 03 (Revision C.02)*, Gaussian, Inc., Wallingford, CT, 2004.
28 J. Cioslowski, *J. Am. Chem. Soc.*, 1989, **111**, 8333.
29 J. Tomasi and M. Persico, *Chem. Rev.*, 1994, **94**, 2027.
30 *Lange's Handbook of Chemistry*, ed. J. A. Dean, McGraw-Hill, 1999, 15th edn.
31 C. Nie, *J. Wuhan Univ. (Nat. Sci. Ed.)*, 2000, **2**, 176.
32 B. J. Coe and S. J. Glenwright, *Coord. Chem. Rev.*, 2000, **203**, 5.
33 J. V. Quagliano and L. E. O. Schubert, *Chem. Rev.*, 1952, **50**, 201.
34 M. Lei, W. Zhang, Y. Chen and Y. Tang, *Organometallics*, 2009, DOI: 10.1021/om900434n.